Jurnal Kejuruteraan 31(2) 2019: 193-199
https://doi.org/10.17576/jkukm-2019-31(2)-02

The Application of Multi-Phase Power Distribution Line with Pure Energy Conversion

Erol Can*
[a]*School of Civil Aviation, Erzincan University, Aircraft Airframe Power Plant, Erzincan, Turkey*
**Corresponding author: can_e@hotmail.com*

Received 27 February 2019, Received in revised form 14 May 2019
Accepted 24 June 2019, Available online 31 October 2019

ABSTRACT

This paper discusses the power transmission of a six-phase power line with a six-phase LPWM inverter. The 20 km long line with six-phase is formed to be fed from the 6-phase multi-level inverter. The structure of the line and the elements of the power line are given in the design phase. After that, mathematical analysis of the power line is done to present information on the line structure and the relationship between the variables of the line. In the application stage, the described line is operating in Matlab Simulink. The input voltage of the line, the voltage of the RC parallel filter on the line and the voltage of the 1MW load on the line are measured. Six phase flux of the power is measured according to b2 and b4 bus points. Harmonic distortion of created voltages is measured. The harmonic distortion of the voltage on the Z_2 impedance is 0.12%. This level of deterioration is well below the international standard of 5% and is an ideal result for loads that need a pure multi-phase magnetic field. 6-phase voltage is measured at 244V amplitude on a 6-phase load with 1 MVA power connecting the secondary side of the transformer. Then, the distortion of this voltage is close to zero. This result is highly desirable for a load on the power line. Based on the results obtained, the power is transmitted over a 20 km long line with high quality successfully.

Keywords: Transmission of a six-phase; six-phase LPWM inverter; a high quality

INTRODUCTION

Energy transmission lines for energy transport and distribution are widely used (Farshad 2019; Fattahi et al. 2019; Khadke et al. 2019 & Quintana et al. 2019). The transport and distribution of the generated energy with a low number of phases may be a problem for multi-phase electrical devices operating with a magnetic field and requiring magnetic fields with different phase angles **(**Tang et al. 2019; González et al. 2019; Pereira et al. 2019; Zhang, Song & Wang 2019). The use of renewable energy sources such as solar energy to feed these lines is a good option because they are clean and easily accessible energy sources **(**Manohar et al. 2019; Nguyen et al. 2019; Shinde et al. 2019; Saxena et al. 2019; Jurasz et al. 2019; Mensah et al. 2019; Ahmed et al. 2019 & Movahedi et al. 2019). Inverter circuits provide that transformation of energy from renewenable energy sources for the power lines. However, while the inverter circuits provide alternating current energy from on the line, they also cause a large number of harmonic distortions (González et al. 2019; Pereira et al., 2019;). In this study, the 20-km long power lines with 6-phase is fed by 14-level inverter with 6-phase. The aim is to provide a low-level harmonic distortion on alternating energy that is transmitted on the six phase distribution line with a 14-level LPWM inverter. So, the line with a large number of phases can provide six phase alternating energy for loads needing a pure multi-phase magnetic field. In the structure, the power line contains serial R-L filter and parallel R-C filter for 6-phases. These filters are located on the primary side of two three-phase transformers with a power of 75KVA in the middle of the line. 14-level inverter with six phases is controlled by linear pulse width modulation. The inverter is a high multi-level inverter structure that will provide the alternating voltage from the direct current. This structure was given for single-phase RL loads and for single-phase asynchronous motor (Can et al. 2017 & Can 2018). The switch of the14-level inverter uses LPWM (Linear Pulse Width Modulation). LPWMs controlling this inverter structure are generated by comparing a 26-triangular signal to a direct signal. In this work, the 14-level LPWM inverter is used for the first time for the 6-phase power line. Therefore, the study is different according to the inverter applications and power line applications in other studies (Manohar et al. 2019; Nguyen et al. 2019; Shinde et al. 2019 & Yusof et al. 2011). In section two, the mathematical model of the power line model is given. In these analyzes, the relationship between the variables in the structure of the power line is revealed. The performance of the circuit in section-3 is made in Matlab Simulink. On the secondary side of the transformers at the power line, there is 1-MVA load and six phase alternating energy source of 40 MVA. On the primary side of the transformer, there are R-C and R-L and the R-L-C circuits representing the 20 km long line. The six-phase alternating voltage with 60° of phase differences is formed with the multilevel vertical voltage pieces on loads when the LPWM inverter feeds the power line. When the power line is operated on Matlab Simulink; the

input voltage of the line, the voltage of the RC parallel filter on the line and the voltage of the 1MW load on the line are measured. Six phase flux of the power is measured according to b2 and b4 bus points. Harmonic distortion of created voltages is measured. The harmonic distortion of the voltage on the Z_2 impedance is 0.12%. This level of deterioration is well below the international standard of 5% and is a very ideal result for loads that need a pure multi-phase magnetic field. 6-phase voltage is measured at 244V amplitude on a 6-phase load with 1 MVA power connecting the secondary side of the transformer. Then, the distortion of this voltage is close to zero. This result is highly desirable for a load on the power line. According to harmonic distortion on the six-phase power line, the results are better than the applications made so far in (Chinmaya et al. 2019; Mukherjee et al. 2019; Shen et al. 2019; Zhao et al. 2019 & Oğuz et. al. 2016). While the load voltages take the exact sinus value while the harmonic distortions support the sinus structure of the voltages and are below the permissible limit of international IEEE standards which is 5%.

CIRCUIT DESCRIPTION

The power distribution line is 200/300 volts, 75 kVA. So, current value can be provided to the power distribution line as well as the voltage value.

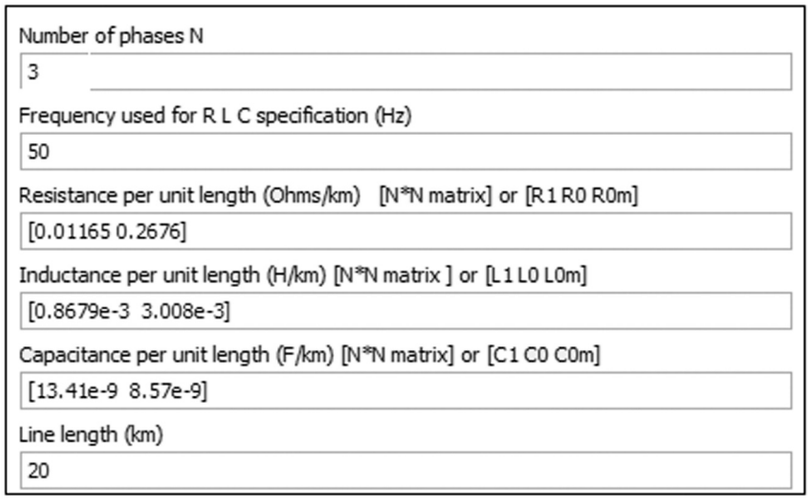

FIGURE 1. The simulation parameters of serial RLC circuit

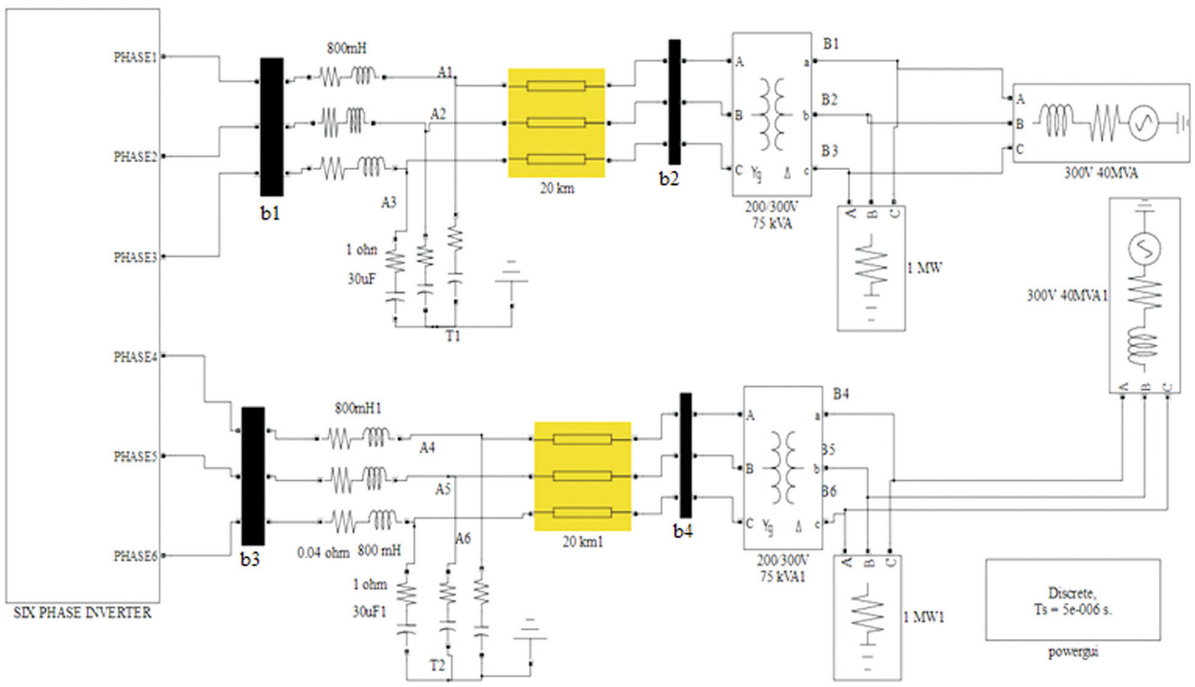

FIGURE 2. The power distribution line with six phase formed by all these circuit elements of the power line

To calculate the equivalent impedance according to the primary side of the power line; the current on each phase of the inverter reaches its own source inputs, regardless of the other phase sources. In the power line, the series R-L-C impedance representing a length of 20 Km, is connected to the parallel R-C impedance. The equivalent of these two impedances is connected in series with the R-L circuit. In the series R-L and serial R-C circuits, the inductive (X_L) and capacitive reactance (Xc) is seen in (1) and (2) respectively. L is inductances, C is capacitance. Frequency is *f*.

$$X_L = 2\pi fL \tag{1}$$

$$X_C = \frac{1}{2\pi fC} \tag{2}$$

In the equation (3), impedance expressions for series R-L and R-C circuits are given respectively in Z_1 and Z_2 while Figure 3 demonstrates the vectorial representation of these impedances.

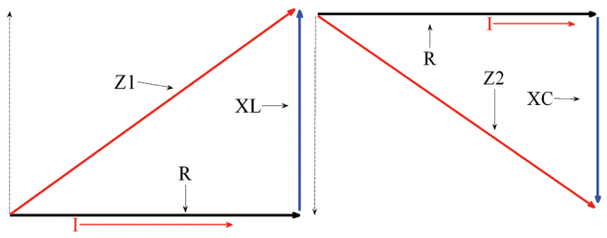

(a) (b)

FIGURE 3. At the power line a) the vector representation of Z_1 impedance b) a) the vector representation of Z_2 impedance

$$Z_1 = \sqrt{R^2 + X_L{}^2} \qquad Z_2 = \sqrt{R^2 + X_C{}^2} \tag{3}$$

In the equation (4), impedance expressions for series R-L-C is given in Z_3 while Fig. 4 shows the vector representation of this impedance.

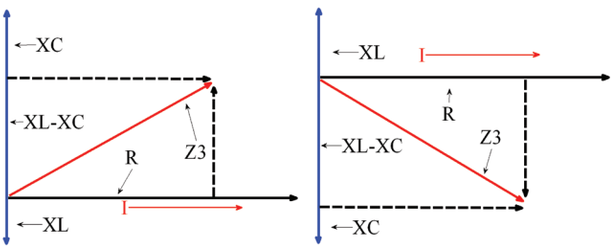

(a) (b)

FIGURE 4. At the power line a) the vector representation of Z_2 impedance while $X_L > X_C$, b) a) the vector representation of Z_3 impedance while $X_C > X_L$

It is important to show that the sizes of XL and XC in vectorial representation to determine whether the circuit is under inductive or capacitive effect.

$$Z_3 = \sqrt{R^2 + (X_L - X_C)^2} \tag{4}$$

Since the difference of $X_L - X_C$ is squared in equation 4, it is not important to state that the X_L is bigger than X_C or the X_C bigger than X_L.

The impedance of the line (Z_B) according to points B4 and B3 can be written as in equation 5.

$$\begin{pmatrix} Z_B = \sqrt{R^2 + X_L{}^2} + \dfrac{1}{\sqrt{R^2 + X_C{}^2}} + \dfrac{1}{\sqrt{R^2 + (X_L - X_C)^2}} \\ Z_B = Z_1 + \dfrac{1}{Z_2} + \dfrac{1}{Z_3} \end{pmatrix} \tag{5}$$

The 14-level voltages with alpha-grade phase difference that the inverter generates are from Eq. 6 to Eq. 11.U is the amplitude of the voltage generated by the inverter. *w* is angular frequency.

The voltages of the six-phase power line are from UP1 to UP6, respectively. Alpha-grade (α) is phase difference.

$$U_{P1} = USinus\ (wt) \tag{6}$$
$$U_{P2} = USinus\ (wt + \alpha) \tag{7}$$
$$U_{P3} = USinus\ (wt + 2\alpha) \tag{8}$$
$$U_{P4} = USinus\ (wt + 3\alpha) \tag{9}$$
$$U_{P5} = USinus\ (wt + 4\alpha) \tag{10}$$
$$U_{P6} = USinus\ (wt + 5\alpha) \tag{11}$$

The currents of the six-phase power line are from IP1 to IP6, respectively. Equalities for the currents are from Eq. 12 to Eq. 17.

$$I_{P1} = \frac{USinus\,(wt)}{Z_1 + \dfrac{1}{Z_2} + \dfrac{1}{Z_3}} \tag{12}$$

$$I_{P2} = \frac{USinus\,(wt + \alpha)}{Z_1 + \dfrac{1}{Z_2} + \dfrac{1}{Z_3}} \tag{13}$$

$$I_{P3} = \frac{USinus\,(wt + 2\alpha)}{Z_1 + \dfrac{1}{Z_2} + \dfrac{1}{Z_3}} \tag{14}$$

$$I_{P4} = \frac{USinus\,(wt + 3\alpha)}{Z_1 + \dfrac{1}{Z_2} + \dfrac{1}{Z_3}} \tag{15}$$

$$I_{P5} = \frac{USinus\,(wt + 4\alpha)}{Z_1 + \dfrac{1}{Z_2} + \dfrac{1}{Z_3}} \tag{16}$$

$$I_{P6} = \frac{USinus(wt + 5\alpha)}{Z_1 + \frac{1}{Z_2} + \frac{1}{Z_3}} \quad (17)$$

The equal impedance values of the six-phase power line can be given from Z_{B1} to Z_{B6}. So, it can be given as in matrix as Equation 18, which gives the relationship of current, voltage and impedance of the six-phase power line.

$$\begin{bmatrix} Z_{B1} \\ Z_{B2} \\ Z_{B3} \\ Z_{B4} \\ Z_{B5} \\ Z_{B6} \end{bmatrix} = \begin{bmatrix} U_{P1} & 0 & 0 & 0 & 0 & 0 \\ 0 & U_{P2} & 0 & 0 & 0 & 0 \\ 0 & 0 & U_{P3} & 0 & 0 & 0 \\ 0 & 0 & 0 & U_{P4} & 0 & 0 \\ 0 & 0 & 0 & 0 & U_{P5} & 0 \\ 0 & 0 & 0 & 0 & 0 & U_{P6} \end{bmatrix} \begin{bmatrix} \frac{1}{I_{P1}} \\ \frac{1}{I_{P2}} \\ \frac{1}{I_{P3}} \\ \frac{1}{I_{P4}} \\ \frac{1}{I_{P5}} \\ \frac{1}{I_{P6}} \end{bmatrix} \quad (18)$$

SIX-PHASE POWER LINE SIMULATION

After the design and mathematical analysis of the power line in the second part, the performance of the power line will be measured in this third section. In Figure 2, the Z_1 impedance of the Series RL circuit at the simulation is 0.04 ohm and 800 mH. In Figure 2, the Z_1 impedance of the series RC circuit connecting as parallel on the phase of the line is 1 ohm and 30×10^{-3}mF. In Figure 2, the Z_1 impedance of the Series RLC of the line is 0.233 ohm 17.358 mH, and 238×10^{-9}F. The simulation of the line is made by Matlab Simulink with a switching time of 5 microseconds. The inverter is a high multi-level inverter structure that will provide the alternating voltage from the direct current. This structure is given for single-phase RL loads and for single-phase asynchronous motor (Can 2018). LPWMs controlling this inverter structure are generated by comparing a 26-triangular signal to a straight signal. In this work, the 14- level LPWM inverter is used for the first time for the 6-phase power line. The voltage supplied by the inverter to the power line is given in Figure 5 and the harmonic distortion of the voltage generated by the inverter is given in Figure 6.

According to Figure 5, the voltages with a 6-phase 60-degree phase different are successfully formed on the power line. The amplitude of these voltages is 187 volts and these volts are 14-level. In Figure 6, the total harmonic distortion of the voltage generated by the 50 Hz frequency is 21.55%. The 6-phase voltages measurement on the Z_2 impedance according to points A are given in Figure 7 and the harmonic distortion of these measured voltage on Z_2 is given in Figure 8.

Figure 7 shows the voltages of 194 volts with six-phase smooth sinus patterns. Because the capacitor in the Z_2 impedance is filtered by a capacitor, amplitude higher than

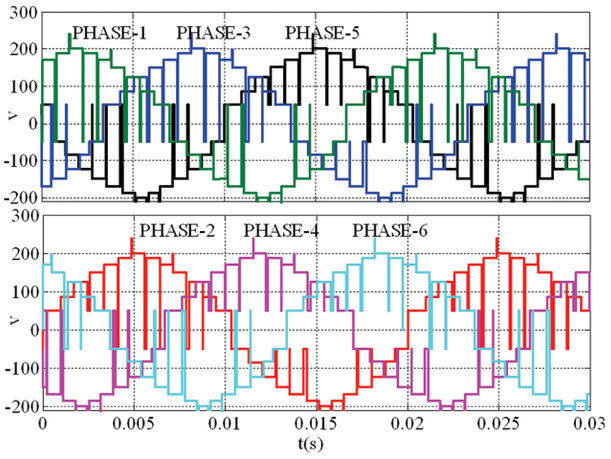

FIGURE 5. The voltage supplied by the inverter to the power line given

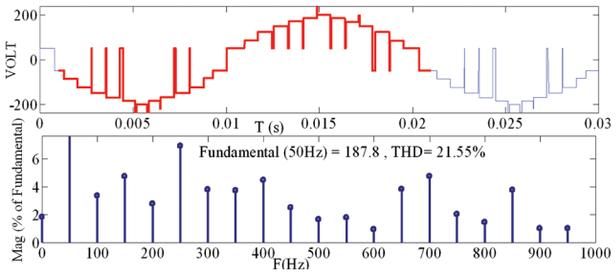

FIGURE 6. The harmonic distortion of the voltage generated by 14-level inverter

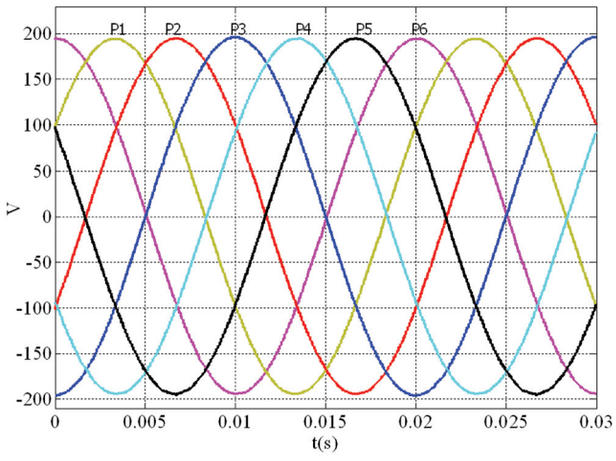

FIGURE 7. The 6-phase voltages measurement on the Z_2 impedances according to points A

the inverter input voltage is measured on the impedance Z_2. The harmonic distortion of the voltage on the impedance Z_2 in Figure 8 is 0.12%. This value is less than 5%, which is an international standard. These results are better than the results of energy conversion studies with many inverters (Mukherjee et al. 2019; Shen et al. 2019 & Zhao et al. 2019).

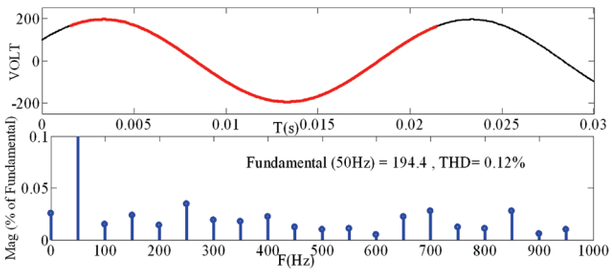

FIGURE 8. Harmonic distortion of the phase voltage on the Z_2 impedance according to points A

The reason for this is that 14- level inverter with LPWM provides input voltages. Figure 9 shows the voltages on a 6-phase 1MW pure resistive load connected to the secondary of the transformer connected to the power line, while figure 10 shows the harmonic distortion of the voltages on a 1MW load.

Figure 9 shows the voltages of 244.8V with six-phase smooth sinus patterns. The harmonic distortion of the voltage on impedance of the 1 MVA load in figure 10 is 0.0001%. This value is less than 5%, which is an international standard.

Figure 10 shows the six-phase current on the Z_B impedance on the primary side of the line. There are six phase fluxes according to b2 and b4 buses point in Figure 11.

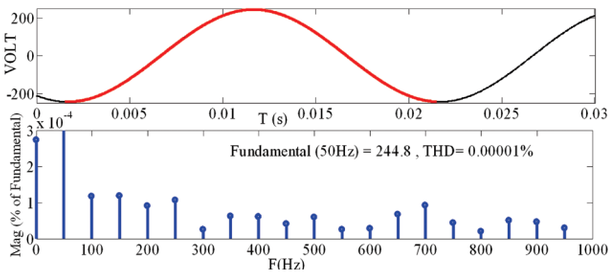

FIGURE 9. The voltages on a 6-phase of 1 mw pure resistive load

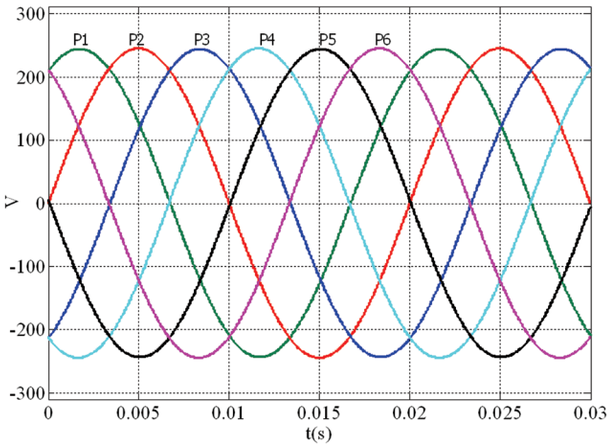

FIGURE 10. The harmonic distortion of the voltages on a 1MW load

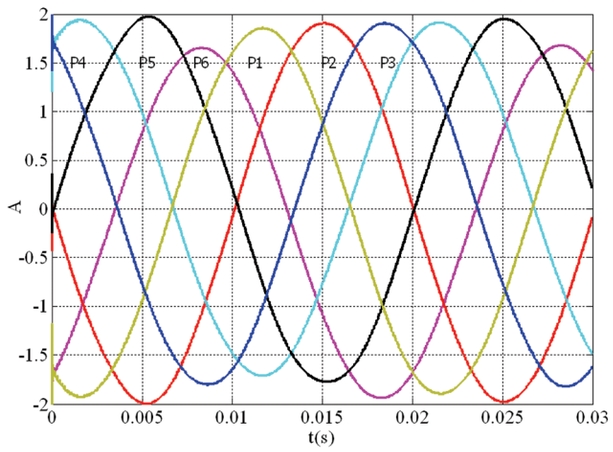

FIGURE 11. The six-phase current on the Z_B impedance on the primary side of the line

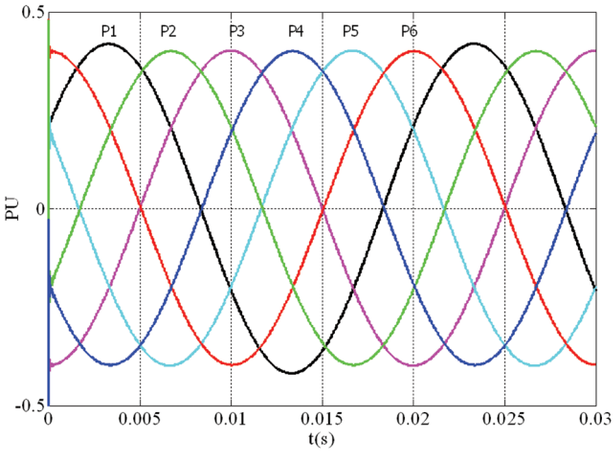

FIGURE 12. Six phase fluxes according to b3 and b4 buses point

The current amplitude in Figure 11 is 1.8A and is in the form of a complete sinus. The flux amplitudes in Figure 12 are 0.4 pu and is in the form of a complete sinus.

The six-phase current, voltage and flux measured in the power line have a smooth sinus and low distortion. Therefore, it is an ideal study for the loads that need to be fed to the multi-phase uniform magnetic fields to be fed on the line. The low voltage level caused by the high level of inverter and loadings leads to large distortions. While the 14-level inverter used in this study provides multi-level voltage with vertical parts to the power line and loads, it provides high quality voltages with suitable filtering process on the voltages it generates.

CONCLUSION

In this study, a 6-phase power line fed by a six-phase 14-level inverter was presented. Firstly, the design and mathematical analysis of the line were made. In accordance with the analysis, the performance of the power line in Matlab Simulink was tested and the performance was measured.

The input voltage of the power line had input voltage 187V amplitude that 14-level inverter provided.

The harmonic distortion value of the output voltage on the inverter was 21.55%. In the voltage measurements on the impedance Z_2, a six phase alternating voltage was measured at 194V amplitude. The harmonic distortion of the voltage on the Z2 impedance was 0.12%. This level of deterioration was well below the international standard of 5%, and was a very ideal result for loads that needing a pure multi-phase magnetic field. The 6-phase voltage at 244V amplitude was measured from a 1 MVA load in this study; the harmonic distortion of the voltage on the impedance of the 1 MVA load was 0.0001%. This value was very less than 5%, which was an international standard. So, this value was very acceptable. According to obtained result, a 6-phase power line fed by a six-phase 14-level inverter with LPWM was successfully performed.

REFERENCES

Ahmed, H.M., Eltantawy, A.B. & Salama, M.M.A. 2019. A reliability-based stochastic planning framework for AC-DC hybrid smart distribution systems. *International Journal of Electrical Power & Energy Systems* 107: 10-18.

Can, E. 2017. Novel high multilevel inverters investigated on simulation. *Electrical Engineering* 99(2): 633-638.

Can, E. 2018. Analysis and Performance with Vertical Divided Multilevel Voltage on Phase of Induction Engine. *Tehnički vjesnik* 25(3): 687-693.

Can, E. & Sayan, H.H. 2017. The increasing harmonic effects of SSPWM multilevel inverter controlling load currents investigated on modulation index. *Tehnički vjesnik* 24(2): 397-404.

Chinmaya, K.A. & Singh, G.K. 2019. Modeling and experimental analysis of grid-connected six-phase induction generator for variable speed wind energy conversion system. *Electric Power Systems Research* 166: 151-162.

Farshad, M. 2019. Detection and classification of internal faults in bipolar HVDC transmission lines based on K-means data description method. *International Journal of Electrical Power & Energy Systems* 104: 615-625.

Fattahi, S., Lavaei, J. & Atamtürk, A. 2019. A bound strengthening method for optimal transmission switching in power systems. *IEEE Transactions on Power Systems* 34(1): 280-291.

González-Torres, I., Miranda, H., Méndez-Barrios, C.F., Espinoza, J. & Cárdenas, V. 2019. Long-length horizons dynamic matrix predictive control for a MMC inverter. *Electric Power Systems Research* 168: 137-145.

Jurasz, J. & Campana, P.E. 2019. The potential of photovoltaic systems to reduce energy costs for office buildings in time-dependent and peak-load-dependent tariffs. *Sustainable Cities and Society* 44: 871-879.

Khadke, P., Patne, N. & Bolisetty, S. 2019. Fault classification and faulty phase selection using symmetrical components of reactive power for ehv transmission line. *Applications of Artificial Intelligence Techniques in Engineering*, 31-42.

Manohar, M., Koley, E. & Ghosh, S. 2019. Enhancing resilience of PV-fed microgrid by improved relaying and differentiating between inverter faults and distribution line faults. *International Journal of Electrical Power & Energy Systems* 108: 271-279.

Mensah, L.D., Yamoah, J.O. & Adaramola, M.S. 2019. Performance evaluation of a utility-scale grid-tied solar photovoltaic (PV) installation in Ghana. *Energy for Sustainable Development* 48: 82-87.

Movahedi, A., Niasar, A.H. & Gharehpetian, G.B. 2019. Designing SSSC, TCSC, and STATCOM controllers using AVURPSO, GSA, and GA for transient stability improvement of a multi-machine power system with PV and wind farms. *International Journal of Electrical Power & Energy Systems* 106: 455-466.

Mukherjee, S., De, S., Sanyal, S., Das, S. & Saha, S. 2019. A 15-level asymmetric H-bridge multilevel inverter using d-SPACE with PDPWM technique. *International Journal of Engineering, Science and Technology* 11(1): 22-32.

Nguyen, H.X., Tsuji, T., Oyama, T. & Uchida, K. 2019. Three phase unbalance elimination in distribution system by optimal inverter dispatch of PCS. *IEEJ Transactions on Power and Energy* 139(1): 13-26.

Oğuz, Y., Şahin, M., Güven, Y. & Tuğcu, H.Z. 2016. Analysing of harmonics affecting the energy quality in opium alkaloids plant's power system. *International Journal of Energy Optimization and Engineering (IJEOE)* 5(4): 26-47.

Pereira, H.A., da Mata, G.L., Xavier, L.S. & Cupertino, A.F. 2019. Flexible harmonic current compensation strategy applied in single and three-phase photovoltaic inverters. *International Journal of Electrical Power & Energy Systems* 104: 358-369.

Quintana-Barcia, P., Dragicevic, T., Garcia, J., Ribas, J. & Guerrero, J. 2019. A distributed control strategy for islanded single-phase microgrids with hybrid energy storage systems based on power line signaling. *Energies* 12(1): 85.

Saxena, A. & Chauhan, D.S. 2019. Rural Electrification Using Microgrids and Its Performance Analysis with the Perspective of Single-Phase Inverter as Its Main Constituent. *Applications of Artificial Intelligence Techniques in Engineering*, 425-437.

Shen, Z. & Jiang, D. 2019. Dead-time effect compensation method based on current ripple prediction for voltage-source inverters. *IEEE Transactions on Power Electronics* 34(1): 971-983.

Shinde, K.D. & Mane, P.B. 2019. Augmenting rooftop solar energy penetration ratio with secondary distribution network using smart inverter for maximum power transfer capacity for subordinate grid-A review. *Energy Sources,*

Part A: Recovery, Utilization, and Environmental Effects 41(6): 713-733.

Tang, D., Yang, X., Yong, J. & Xu, W. 2019. Active method for mitigation of induced voltage in integrated energy systems. *Applied Energy* 235: 553-563.

Yusof, Y. & Rahim, A.N. 2011. Comparative study between spwm control techniques thipwm for pwm-vsi using mathematical modeling and simulation. *Jurnal Kejuruteraan* 23: 17-26.

Zhang, M., Song, B. & Wang, J. 2019. Circulating current control strategy based on equivalent feeder for parallel inverters in islanded microgrid. *IEEE Transactions on Power Systems* 34(1): 595-605.

Zhao, J., Hua, M., Liu, T. & Yu, T. 2019. Study on topology and control strategy of high-precision and wide-range hybrid converter for photovoltaic cell simulator. *Energies* 12(1): 39.